

---

## Electronic Supplementary Information

# Fibrillation Kinetics of A $\beta$ (1-40) Peptide Depend on Surface Curvature at Nano-Bio Interfaces

Guanbin Gao,<sup>a</sup> Mingxi Zhang,<sup>a</sup> Dejun Gong,<sup>b</sup> Rui Cheng,<sup>b</sup> Xuejiao Hu,<sup>a</sup> and Taolei Sun<sup>a, b, \*</sup>

<sup>a</sup> State Key Laboratory of Advanced Technology for Materials Synthesis and Processing, Wuhan University of Technology, Wuhan, People's Republic of China. E-mail: [suntl@whut.edu.cn](mailto:suntl@whut.edu.cn)

<sup>b</sup> School of Chemistry, Chemical Engineering and Life Science, Wuhan University of Technology, 122 Luoshi Road, Wuhan 430070, People's Republic of China. E-mail: [suntl@whut.edu.cn](mailto:suntl@whut.edu.cn)

## Content

### 1. *Supplementary Figures and relevant discussion*

1.1 FT-IR spectra of GSH, AuNCs, AuNPs1, 2 and 3 (Fig. S1)

1.2 Histogram of diameter probability distribution for AuNCs, AuNPs1, 2 and 3 (Fig. S2)

1.3 AFM image of QCM crystal without GSH modification after QCM experiment and A $\beta$ (1-40) deposited on mica substrates after incubation for 24 hours (Fig. S3)

1.4 Effect of High concentration of AuNPs1, 2, 3 and AuNCs on ThT Fluorescence Quenching (Fig. S4)

1.5 Dependence of  $t_{1/2}$  and  $t_{1/2}/t_{1/2, A\beta}$  of A $\beta$ (1-40) peptide fibrillation on the concentrations of AuNCs, AuNPs1, 2 and 3 (Fig. S5)

1.6 ThT fluorescence dynamic monitoring curves with error bar in the presence of AuNPs1, 2, 3 and AuNCs with different concentrations (Fig. S6-9)

**1.7** Fibrillation kinetics for A $\beta$ (1-40) in the presence of AuNPs1, AuNPs2, AuNPs3 and AuNCs with same total surface area (Fig. S10)

**1.8** AFM images of amyloid fibrils co-incubating with AuNPs1, 2, 3 and AuNCs for different hours (Fig. S11-12)

## 1. Supplementary Figures and relevant discussion

### 1.1 FT-IR spectra of GSH, AuNCs, AuNPs1, 2 and 3

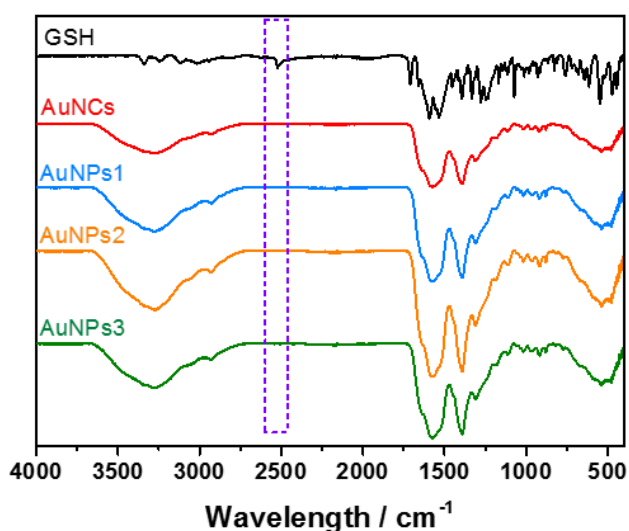


**Fig. S1** FT-IR spectra of GSH (black curve), AuNCs (red curve), AuNPs1 (blue curve), AuNPs2 (orange curve) and AuNPs3 (green curve).

As shown in Fig. S1, compare GSH with AuNCs, AuNPs1, AuNPs2 and AuNPs3, the disappear of -S-H stretching vibration absorption ( $2600\text{-}2500\text{ cm}^{-1}$ ) in FT-IR spectra of AuNCs, AuNPs1, AuNPs2 and AuNPs3 indicate that GSH were successfully grafted onto them.

### 1.2 Histogram of diameter probability distribution for AuNCs, AuNPs1, 2 and 3

Fig. S2 show the histogram of diameter probability distribution for AuNCs, AuNPs1, 2 and 3 according to the high resolution images of AuNCs and three kinds of AuNPs taken by TEM. The

statistical data show that their average diameter are  $1.9 \pm 0.7$  nm (AuNCs),  $36.0 \pm 3.0$  nm (AuNPs1),  $18.1 \pm 3.0$  nm (AuNPs2), and  $6.0 \pm 2.0$  nm (AuNPs3), respectively. More than 1000 of AuNPs1, AuNPs2, AuNPs3 and AuNCs are randomly selected for recording, respectively.

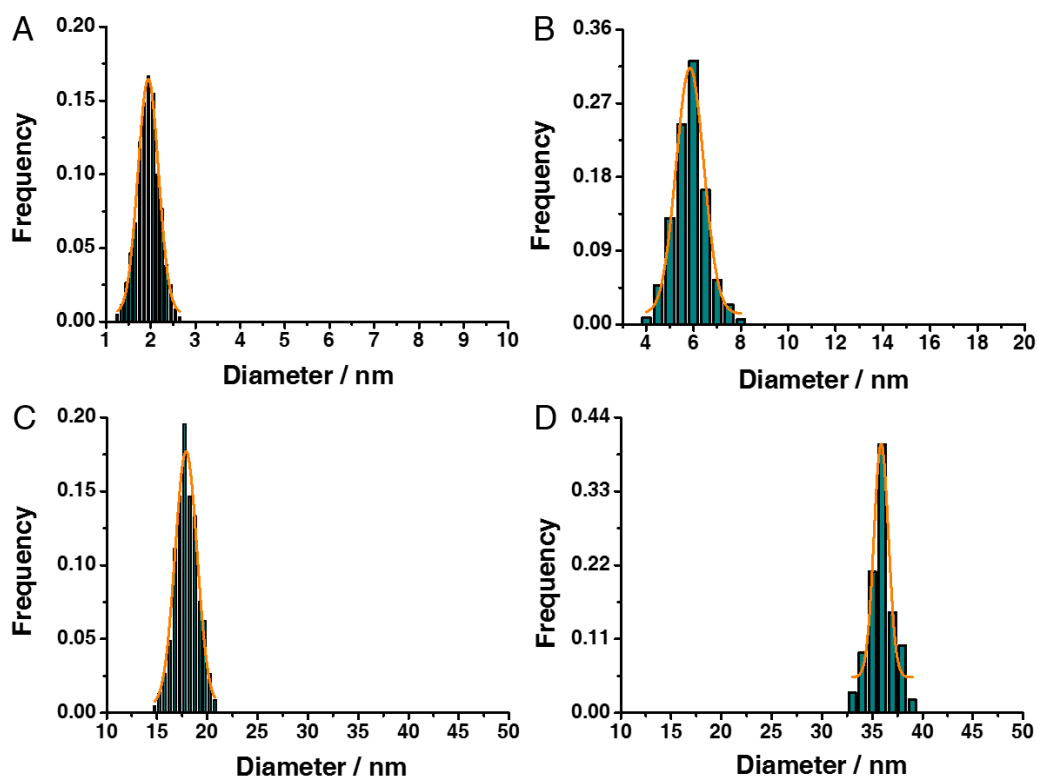


**Fig. S2** Histogram of diameter probability distribution for AuNCs (A), AuNPs3 (B), AuNPs2 (C) and AuNPs1 (D).

### 1.3 AFM image of QCM crystal without GSH modification after QCM experiment and $A\beta(1-40)$ deposited on mica substrates after incubation for 24 hours

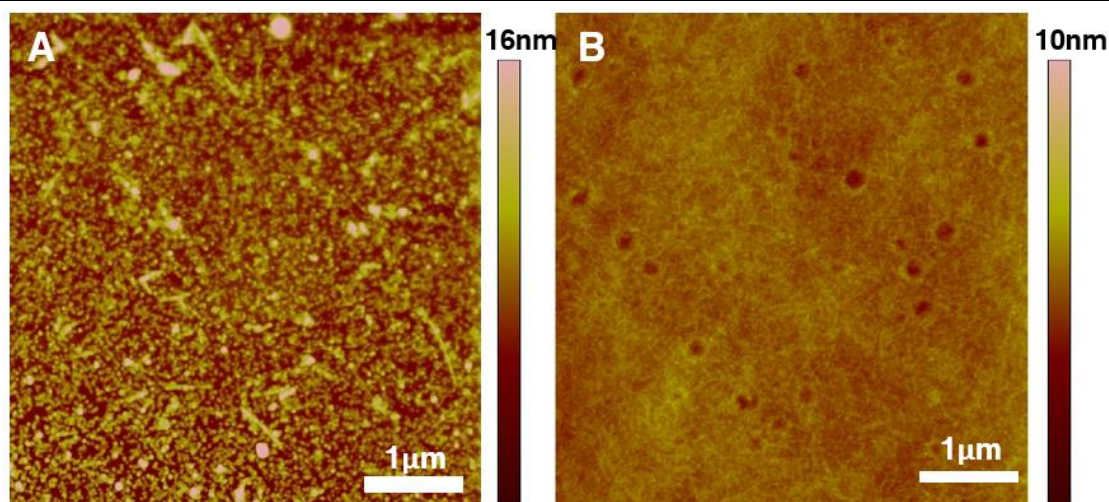


**Fig. S3** (A) AFM image of QCM crystal without GSH modification after QCM experiment; (B) AFM image of 10  $\mu\text{M}$   $\text{A}\beta(1-40)$  deposited on mica substrates after incubation in PBS for 24 hours.

#### 1.4 Effect of High concentration of AuNPs1, 2, 3 and AuNCs on ThT

##### Fluorescence Quenching

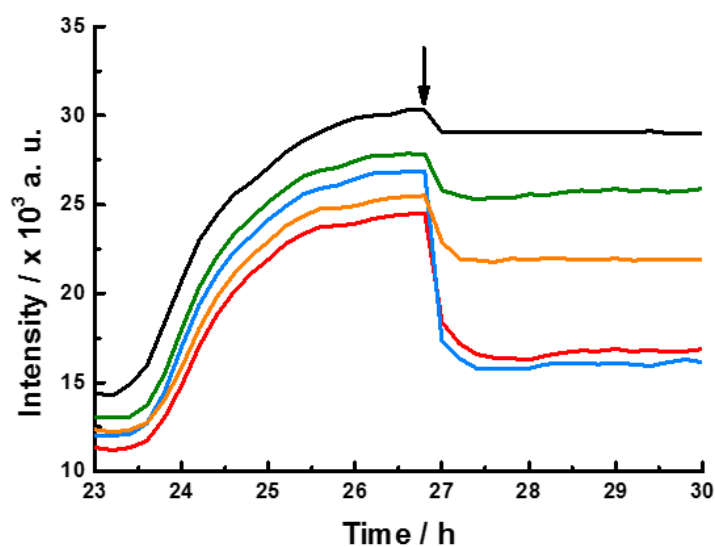


**Fig. S4** Fibrillation kinetics (ThT assay) for 20  $\mu\text{M}$   $\text{A}\beta(1-40)$  incubated in 200  $\mu\text{L}$  PBS (10 mM, pH = 7.4) at 37  $^{\circ}\text{C}$ . 50  $\mu\text{L}$   $\text{H}_2\text{O}$  (black curve), AuNPs1 (blue curve), AuNPs2 (red curve), AuNPs3 (orange curve) and AuNCs (green curve) with a concentration of 100 ppm were added into the mixed solution at the beginning of the 27<sup>th</sup> hour.

Fig. S4 showed that the addition of H<sub>2</sub>O, AuNPs1, 2, 3 and AuNCs with a high concentration of 100 ppm after 27 h of incubation made the ThT fluorescence intensity decrease in varying degrees. For the addition of H<sub>2</sub>O, the small decline (about 4.3%) of ThT fluorescence intensity can be explained by the dilutions of A $\beta$ (1-40). For three AuNPs, the decline degree of ThT fluorescence intensity is increasing with the diameter of the AuNPs (AuNPs3: 15.7%, AuNPs2: 33.9%, AuNPs1: 41.1%). These can be explained by the surface SPR effect of AuNPs partially quench the fluorescence of ThT, and the fluorescence quench effect increases monotonically with increasing nanoparticle diameters and concentration,<sup>3</sup>. For the addition of AuNCs, the decline (about 7.2%) of ThT fluorescence intensity is smaller than all AuNPs, but slightly bigger than H<sub>2</sub>O. This is because AuNCs do not have SPR effect, and thus will not induce the quench of ThT fluorescence. These results indicate that though the intensities of ThT fluorescence in the presence of high concentration of AuNPs1 and 2 were lower than that of the A $\beta$ (1-40) peptide alone (Fig. 3a and b, Fig. S6-7), thus in these figures, the decrease of fluorescent intensity should not be attributed to the suppression of fibrillation. For AuNPs3, the fluorescence quench effect is obviously smaller than AuNPs1 and 2, 100 ppm AuNPs3 only made the intensity of ThT fluorescence decrease 15.7%. So the decrease of fluorescence intensity in Fig. 3c and Fig. S8 should partially be attributed to the suppression against A $\beta$ (1-40) fibrillation. Since AuNCs do not have SPR effect, and thus will not induce the quench of ThT fluorescence, the decrease of fluorescence intensity in Fig. 3d and Fig. S9 should mainly be attributed to the inhibition against A $\beta$ (1-40) fibrillation. Therefore, for AuNPs, it's better to study their influence on A $\beta$ (1-40) fibrillation by the time when growth stage appears.

### **1.5 Dependence of $t_{1/2}$ and $t_{1/2}/t_{1/2, A\beta}$ of A $\beta$ (1-40) peptide fibrillation on the**

## concentrations of AuNCs, AuNPs1, 2 and 3

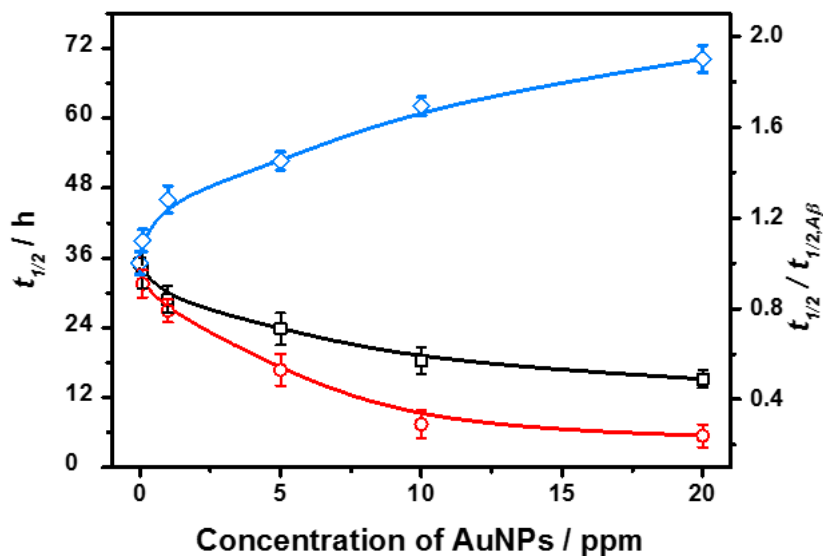


**Fig. S5** Dependence of the half times ( $t_{1/2}$ , left Y-axis) and  $t_{1/2}/t_{1/2, A\beta}$  (right Y-axis) of A $\beta$ (1-40) peptide fibrillation on the concentrations of AuNPs1 (red), AuNPs2 (black) and AuNPs3 (blue).

The overall effect of the AuNPs on the A $\beta$ (1-40) fibrillation kinetics was evaluated by using  $t_{1/2}$ , which refers to the time when 50% of the monomers are transferred into fibrils in the fibrillation process. For AuNPs with larger diameters (AuNPs1 and AuNPs2),  $t_{1/2}$  showed a progressive decrease with the increasing of AuNPs concentration, which arrived at a plateau at  $\sim 10$  ppm and 15 ppm (Fig. S5), respectively. For example, the maximum effect caused by the AuNPs1 and 2 leads to the decrease of  $t_{1/2}$  to 7 h and 14 h, respectively, which are equal to 20% and 50% of the value of  $t_{1/2}$  for A $\beta$ (1-40) peptide alone ( $t_{1/2, A\beta}$ ). In contrast, for AuNPs with smaller diameter (AuNPs3),  $t_{1/2}$  showed a significant increase as a function of AuNPs concentration. And such AuNPs3 with concentrations larger than 10 ppm can almost delay the fibrillation of 20  $\mu\text{mol}\cdot\text{L}^{-1}$  A $\beta$ (1-40) peptides more than 24 hours.

### 1.6 ThT fluorescence dynamic monitoring curves with error bar in the presence of AuNPs1, 2, 3 and AuNCs with different concentrations

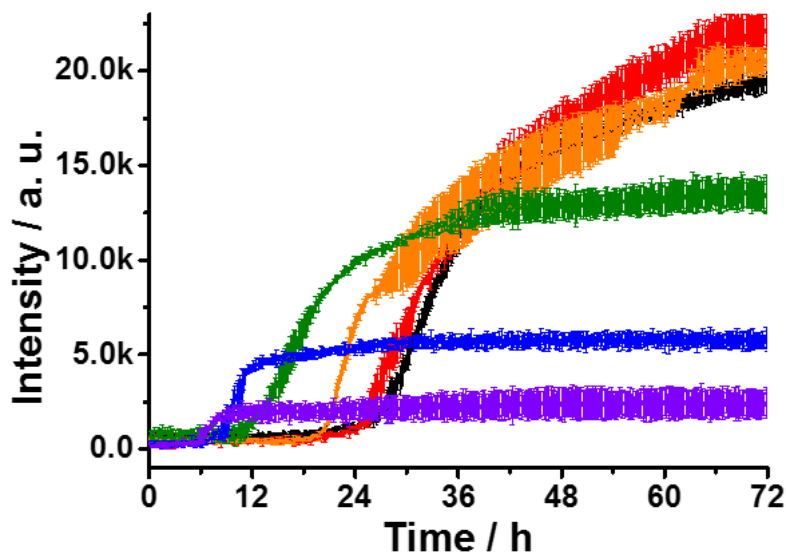


**Fig. S6** Fibrillation kinetics (ThT assay) for  $20 \mu\text{mol}\cdot\text{L}^{-1}$   $\text{A}\beta(1-40)$  in  $10 \text{mmol}\cdot\text{L}^{-1}$  PBS ( $\text{pH} = 7.4$ ) in the presence of AuNPs1 with different concentrations. The colors of the curves represented different concentrations of AuNPs1, black: 0, red: 0.1 ppm, orange: 1 ppm, green: 5 ppm, blue: 10 ppm, purple: 20 ppm; each curve displayed the average data of six parallel experiments. In all panels, error bars show the standard deviations of the averaged data sets. Experiments were repeated three times, and each time the experiment was carried out in triplicate.

As shown in the Fig. S6, due to the fluorescence quench effect increases monotonically with increasing nanoparticle concentration,<sup>3</sup> the intensities of ThT fluorescence in the presence of high concentration of AuNPs1 were lower than that of  $\text{A}\beta(1-40)$  peptide alone. However, though the intensities of ThT fluorescence in the presence of high concentration of AuNPs1 were lower (Fig. S6), the AFM (Fig. S11C and D) and TEM (Fig. 4A) images showed that the amounts of amyloid fibrils forming in the presence of such AuNPs1 were more than the  $\text{A}\beta(1-40)$  peptide alone (Fig. S11A and B) after incubation for 48 hours.

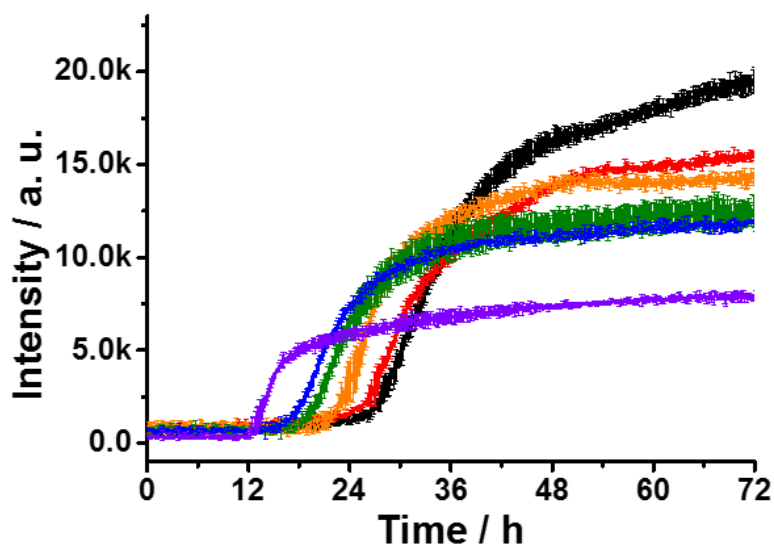


**Fig. S7** Fibrillation kinetics (ThT assay) for  $20 \mu\text{mol}\cdot\text{L}^{-1}$   $\text{A}\beta(1-40)$  in  $10 \text{mmol}\cdot\text{L}^{-1}$  PBS ( $\text{pH} = 7.4$ ) in the presence of AuNPs2 with different concentrations. The colors of the curves represented different concentrations of AuNPs2, black: 0, red: 0.1 ppm, orange: 1 ppm, green: 5 ppm, blue: 10 ppm, purple: 20 ppm; each curve displayed the average data of six parallel experiments. In all panels, error bars show the standard deviations of the averaged data sets. Experiments were repeated three times, and each time the experiment was carried out in triplicate.

As shown in the Fig. S7, due to the fluorescence quench effect, the intensities of ThT fluorescence in the presence of high concentration of AuNPs2 were also lower than that of  $\text{A}\beta(1-40)$  peptide alone. As with AuNPs1, though the intensities of ThT fluorescence in the presence of high concentration of AuNPs2 were lower (Fig. S7), the AFM (Fig. S11E and F) and TEM (Fig. 4B) images showed that the amounts of amyloid fibrils forming in the presence of these AuNPs2 were also more than the  $\text{A}\beta(1-40)$  peptide alone (Fig. S11A and B) after incubation for 48 hours.



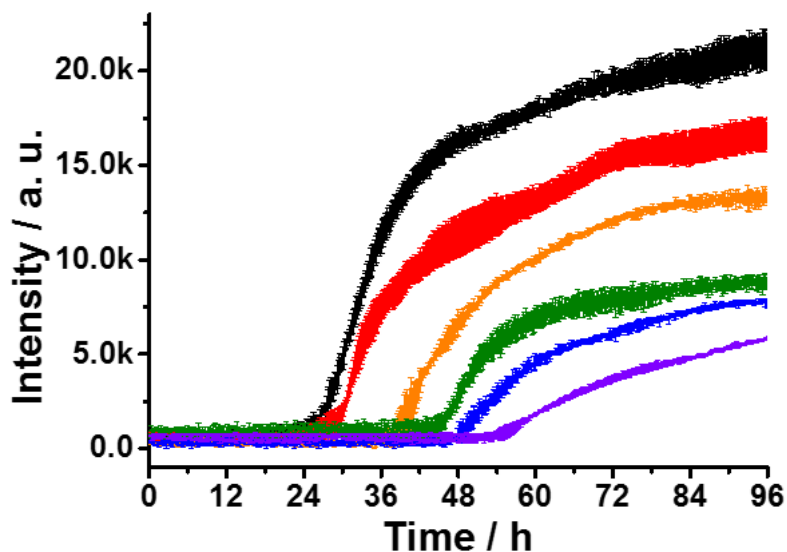


**Fig. S8** Fibrillation kinetics (ThT assay) for  $20 \mu\text{mol}\cdot\text{L}^{-1}$   $\text{A}\beta(1-40)$  in  $10 \text{mmol}\cdot\text{L}^{-1}$  PBS ( $\text{pH} = 7.4$ ) in the presence of AuNPs3 with different concentrations. The colors of the curves represented different concentrations of AuNPs3, black: 0, red: 0.1 ppm, orange: 1 ppm, green: 5 ppm, blue: 10 ppm, purple: 20 ppm; each curve displayed the average data of six parallel experiments. In all panels, error bars show the standard deviations of the averaged data sets. Experiments were repeated three times, and each time the experiment was carried out in triplicate.

As shown in the Fig. S8, the retardation effects also depended on the concentration of such AuNPs3 within the range studied here. With the increasing of AuNPs3 concentration, the starting time of growth phase (i.e. fibril formation process) significantly delayed. Due to the fluorescence quench effect caused by AuNPs3 is not as strong as the AuNPs 1 and 2, the decrease of fluorescence intensity here should mainly be attributed to the inhibition against  $\text{A}\beta(1-40)$  fibrillation. And for this AuNPs3, the addition of them with a concentration of 20 ppm can result in a delay of growth phase for more than 50 hours maximally.

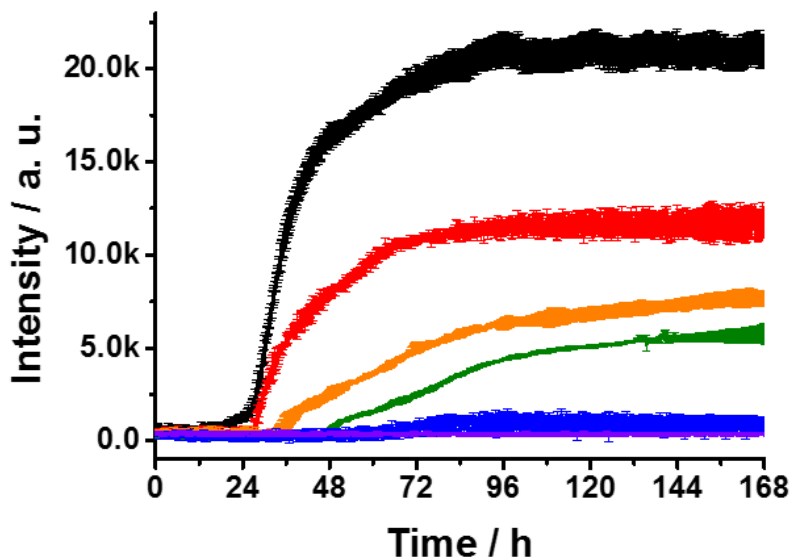


**Fig. S9** Fibrillation kinetics (ThT assay) for  $20 \mu\text{mol}\cdot\text{L}^{-1}$   $\text{A}\beta(1-40)$  in  $10 \text{mmol}\cdot\text{L}^{-1}$  PBS ( $\text{pH} = 7.4$ ) in the presence of AuNCs with different concentrations. The colors of the curves represented different concentrations of AuNCs, black: 0, red: 0.1 ppm, orange: 1 ppm, green: 5 ppm, blue: 10 ppm, purple: 20 ppm; each curve displayed the average data of six parallel experiments. In all panels, error bars show the standard deviations of the averaged data sets. Experiments were repeated three times, and each time the experiment was carried out in triplicate.

As shown in the Fig. S9, the retardation effects also depended on the concentration of such AuNCs within the range studied here. Since AuNCs do not have SPR effect, and thus will not induce the quench of ThT fluorescence, the decrease of fluorescence intensity should mainly be attributed to the inhibition against  $\text{A}\beta(1-40)$  fibrillation. And amazingly, when the concentration increased to 10 ppm, the fluorescence intensity remained at the background level and the growth phase did not appear even after 168 hours of incubation

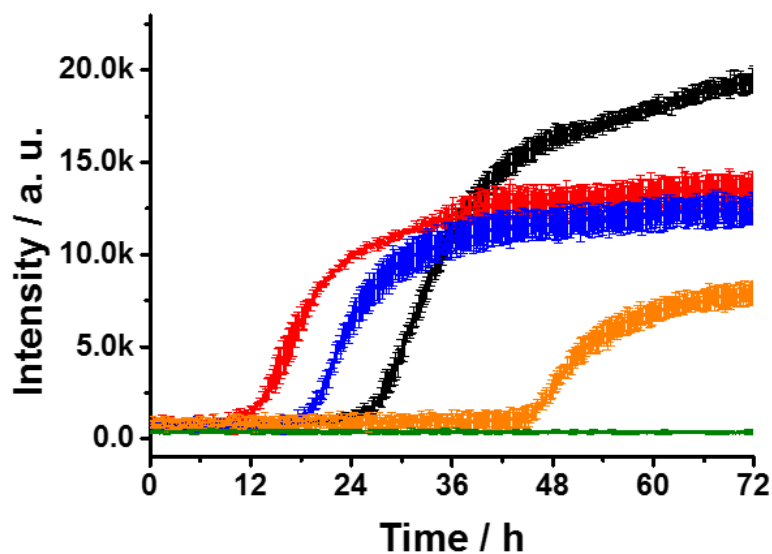
### **1.7 Fibrillation kinetics for $\text{A}\beta(1-40)$ in the presence of AuNPs1, AuNPs2, AuNPs3 and AuNCs with same total surface area.**

To better understand the surface curvature effect of nano-bio interfaces, the fibrillation kinetics

of A $\beta$ (1-40) peptides was investigated in the presence of AuNPs1, 2, 3 and AuNCs with same total surface area (Fig. S10), which provide equal numbers of binding sites for A $\beta$ (1-40) molecules binding to. Due to the different surface-to-volume ratios of AuNPs, the numbers of binding sites on individual particle surface would increase with the increasing of curvature radius. The concentrations of AuNPs in solutions were determined by the Equation 1,  $S_T$  is the total surface area of all AuNPs spheres in solution;  $V$  is the volume of solution;  $d$  is the diameter of AuNPs. So, in the same  $S_T$ , with the surface curvature radius of AuNPs increasing, the molarity of AuNPs is reduced.

$$C = \frac{S_T}{\pi V d^2}$$

Equation 1



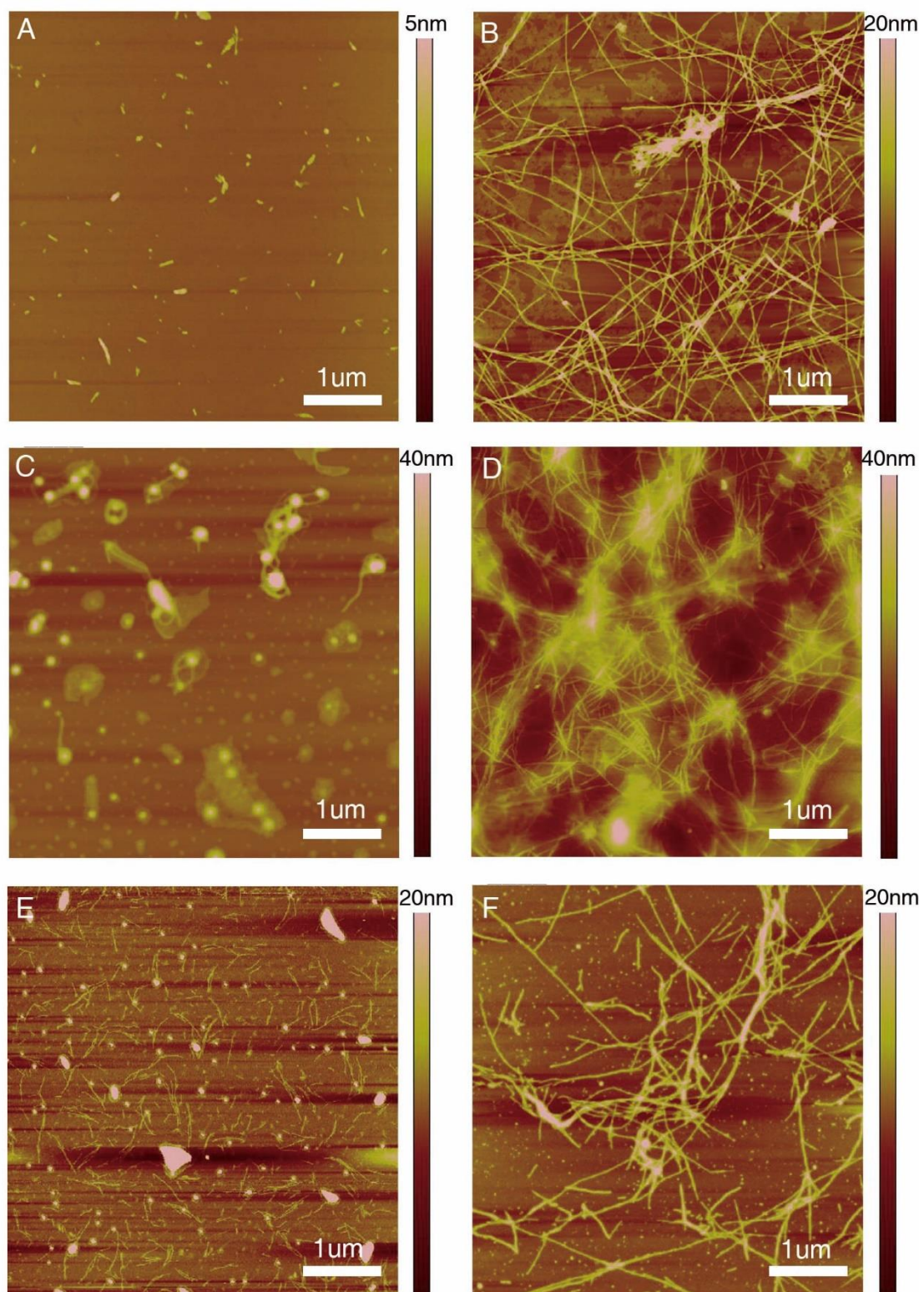
**Fig. S10** Fibrillation kinetics for 20  $\mu\text{mol}\cdot\text{L}^{-1}$  A $\beta$ (1-40) in 10  $\text{mmol}\cdot\text{L}^{-1}$  PBS (pH 7.4) in the presence of no additives (black), AuNPs1 (red), AuNPs2 (blue), AuNPs3 (orange) and AuNCs (green) with same total surface area. Each curve is the average value of six parallel experiments.

Fig. S10 showed the growth curves of A $\beta$ (1-40) in the absence and presence of AuNPs1, AuNPs2, AuNPs3 and AuNCs with same total surface area. Compare to the growth curve of fibrils

with no additives (black curve), the addition of AuNPs1 and 2 can bring forward the growth phase for 12 and 6 hours, respectively. In contrast, the addition of AuNPs3 delays this process nearly 24 hour. To our surprise, the addition of AuNCs (green curve) led to no increase in ThT fluorescence in the first 72 hours. Above result definitely indicate the size effect of AuNPs and AuNCs on the fibrillation kinetics of A $\beta$ (1-40) peptide. Under the same concentration, for nano-bio interfaces with larger surface curvature radii (AuNPs1 and 2), the promotion effect will be enhanced with the increase of surface curvature radius, for nano-bio interfaces with smaller surface curvature radii (AuNPs3 and AuNCs), the retardation effect will increase with the decrease of the surface curvature radius. It must be noted here that the concentrations of four AuNPs here were selected to represent the large-scale trend according to experiments. Due to the fluorescence quench effect increases monotonically with increasing nanoparticle diameter,<sup>3</sup> the intensities of ThT fluorescence in the presence of AuNPs1 and 2 were lower than that of the A $\beta$ (1-40) peptide alone.

### **1.8 AFM images of amyloid fibrils co-incubating with AuNPs1, 2, 3 and AuNCs for different hours (Fig. S11-12)**

AFM images provided another proof for the mechanism about that AuNPs with larger surface curvature radii (AuNPs1 and 2) can provide more binding sites at each nanoparticle surface to adsorb more A $\beta$ (1-40) monomers onto the corresponding nano-bio interfaces (Fig. S11C and E). The increase of local concentration of A $\beta$ (1-40) peptides obviously accelerated the amyloid fibrillation process, which resulted in that the mature amyloid fibrils forming in the presence of AuNPs with larger curvature radii (Fig. S11D and F) were even more than the A $\beta$ (1-40) peptide alone (Fig. S11B) after incubation for 48 hours.



**Fig. S11** A and B are AFM images of A $\beta$ (1-40) peptide on mica plate after incubation 12 and 48 hours. C and D are AFM images of A $\beta$ (1-40) on mica plate after co-incubating with AuNPs1 for 12 and 48 hours. E and F are AFM images of A $\beta$ (1-40) on mica plate after co-incubating with



AuNPs2 for 18 and 48 hours.

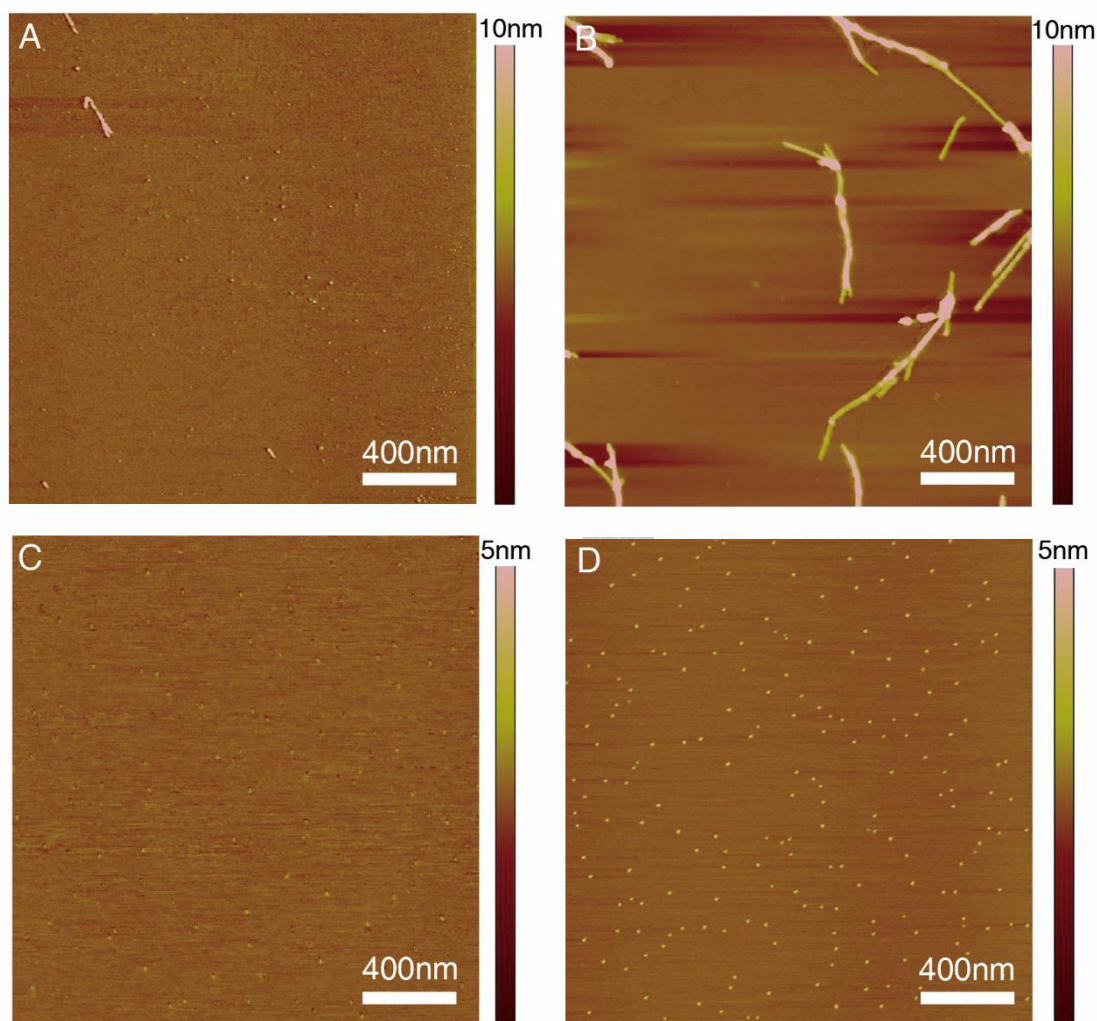


**Fig. S12** A and B are AFM images of A $\beta$ (1-40) on mica plate after co-incubating with AuNPs3 for 36 and 72 hours. C and D are AFM images of A $\beta$ (1-40) on mica plate after co-incubating with AuNCs for 36 and 72 hours.

These AFM images provided the mechanism about that a single nanoparticle with smaller curvature radius can only provide very limited amounts of binding sites to adsorb a few A $\beta$ (1-40) molecules onto its surface (Fig. S12A and C). However, plenty of such decentralized A $\beta$ (1-40)-bound AuNPs existing in system would prevent the rising of local concentration of A $\beta$ (1-40) peptides, which would lead to A $\beta$ (1-40) monomers self-associate with relatively more restraints in

solution. So, in the presence of AuNPs3 and AuNCs, only few short fibrils (Fig. S12B and D) were observed.